CrystEngComm

PAPER

Constructing nanosized polyanions with diverse structures by the self-assembly of W/Nb mixed-addendum polyoxometalate and lanthanide ion†

Shu-Jun Li,[a] Shu-Xia Liu,*[a] Na-Na Ma,[b] Yong-Qing Qiu,[b] Jun Miao,[a] Cong-Cong Li,[a] Qun Tang[a] and Lin Xu[a]

The reaction activity of W/Nb mixed-addendum POMs towards lanthanide has been demonstrated by experimental and computational methods. Utilizing the nucleophilicity of $O_t(Nb)$ (O_t: terminal oxygen), six Nb–O–Eu bridge-based POMs with different structures have been isolated by the reactions of $\{GeW_9Nb_3O_{40}\}$ and lanthanide ions Eu^{3+} under different conditions, including a dimmer $Cs_3K_4[(Ge_2W_{18}Nb_6O_{78})Eu(H_2O)_4] \cdot 23H_2O$ (**1**), three tetramers $Cs_8K_9[(Ge_4W_{36}Nb_{12}O_{156})Eu(H_2O)_3] \cdot 25H_2O$ (**2**), $Cs_{12}K_2[Cs(GeW_9Nb_3O_{40})_4(SO_4)Eu_5(H_2O)_{36}] \cdot 61H_2O$ (**3**), $Cs_{12.5}K_{1.5}[Cs_2(GeW_9Nb_3O_{40})_4Eu_4(H_2O)_{22}] \cdot 28H_2O$ (**4**), a one-dimensional compound $Cs_{11.5}[(GeW_9Nb_3O_{40})_4Eu_{5.5}(H_2O)_{26}] \cdot 24H_2O$ (**5**), and a two-dimensional compound $CsK_{2.25}[GeW_9Nb_3O_{40}Eu_{1.25}(H_2O)_{12}] \cdot 8H_2O$ (**6**). In the polyanions of **1–6** (**1a–6a**), all the Eu^{III} atoms are selectively bonded to $O_t(Nb)$ of $\{GeW_9Nb_3O_{40}\}$ fragments, indicating the high nucleophilicity of $O_t(Nb)$. The Density Functional Theory (DFT) calculation on anion $[GeW_9Nb_3O_{40}]^{7-}$ further approves this. Comparing with the (Nb)O–Eu bonds, the formation of Nb–O–Nb bridges needs stronger acidity. Thus, weaker acidity (pH>1.5) is favorable to the former. The Cs^+ cation plays an important templating role in the formation and stability of polyanions **1a–5a**. The photoluminescence behaviors of **1** and **2** have been investigated and compound **1** exhibits selective luminescence response to malonic acid.

Introduction

The design and synthesis of lanthanide-containing polyoxometalates (POMs) is of contemporary interest, owing to their physicochemical properties and applications in catalysis, magnetochemistry, electrochemistry and luminescence.[1,2] Since the first lanthanide-containing polytungstate (POT) reported in 1971,[3] there has been rapid development for the lanthanide-containing POTs.[4] The synthesis strategy of these compounds mainly focused on the condensation of lanthanide cations and lacunary POTs which have highly basic oxygen atoms and can be considered as inorganic multidentate ligands.[5] We consider that the combination of polyoxoniobates (PONs) and lanthanide should also be conceivable because of the high surface charge of PONs. For example, the Lindqvist-Type isopolyoxoanion $[Nb_6O_{19}]^{8-}$ has the greatest surface charge of all POMs, and the Keggin-Type heteropolyniobates $[TNb_{12}O_{40}]^{16-}$ (T = Si, Ge)

reported by Nyman *et al.* have the highest negative charge compared with the closed-shell (plenary) and typical lacunary Keggin anions. This character makes PONs have sticky surfaces and display an unusual tendency of strongly associating with other species, including protons, alkali metal ions, and transition metal complexes.[6,7] Though possessing great potential, the introduction of lanthanide to PONs has been strictly prevented by the basic condition that PONs need to keep stable. So far, only one example of lanthanide-containing PON ($\{[Eu_3O(OH)_3(OH_2)_3]_2Al_2(Nb_6O_{19})_5\}^{26-}$) has been reported under basic condition by Yamase *et al.* in 1994.[8]

We realize that Nb/W mixed-addendum POMs will be suitable candidates for actualizing the combination of PONs and lanthanide. Firstly, they can exist in a broad pH range (acidic and neutral).[9] Secondly and importantly, the substitution of Nb^V for W^{VI} will increase the charge of the whole polyoxoanion and endow the polyoxoanion with high reactivity as a result of the enhanced basicity and nucleophilicity of the oxygen atoms, especially those bound to Nb $\{O(Nb)\}$.[10] Therefore the basic O(Nb) atoms are expected to be active towards oxophilic lanthanide ions.

Several Nb/W mixed-addendum polyanions, including Lindqist, Keggin and Dawson structure-types have been reported.[9,11] Utilizing the nucleophilic O(Nb), a number of Nb/W mixed-addendum POMs-supported organometallic complexes with excellent catalytic properties have been isolated in organic

[a] Key Laboratory of Polyoxometalate Science of the Ministry of Education, College of Chemistry, Northeast Normal University, Changchun, Jilin, 130024, China. E-mail: liusx@nenu.edu.cn; Fax: + 86-431-85099328; Tel: + 86-431-85099328
[b] Institute of Functional Material Chemistry, College of Chemistry, Northeast Normal University, Changchun, Jilin, 130024, China
† Electronic supplementary information (ESI) available: Additional structural figures, DFT calculations, photoluminescence spectra, IR spectra and TG curves. See DOI: 10.1039/c1ce06225e

solvent.[12] However, the field of combining Nb/W mixed-addendum POMs and lanthanides is still unexplored. If the closed-shell Nb/W mixed-addendum POMs are approved to be indeed active towards lanthanide, how about their reactivity compared with the well understood lacunary POTs? Moreover, as a class of building blocks, can the mixed-addendum POMs replace the role that the well studied lacunary POTs played on the stage of POMs chemistry in the past thirty years? These questions inspire us to investigate intensively in this area.

Herein, utilizing the assembly of triniobium-substituted germanotungstate and lanthanide ion Eu^{3+} in aqueous solution, we isolated six novel compounds with unprecedented architectures: $Cs_3K_4[(Ge_2W_{18}Nb_6O_{78})Eu(H_2O)_4]\cdot23H_2O$ (**1**), $Cs_8K_9[(Ge_4W_{36}Nb_{12}O_{156})Eu(H_2O)_3]\cdot25H_2O$ (**2**), $Cs_{12}K_2[Cs(GeW_9Nb_3O_{40})_4(SO_4)Eu_5(H_2O)_{36}]\cdot61H_2O$ (**3**), $Cs_{12.5}K_{1.5}[Cs_2(GeW_9Nb_3O_{40})_4Eu_4(H_2O)_{22}]\cdot28H_2O$ (**4**), $Cs_{11.5}[(GeW_9Nb_3O_{40})_4Eu_{5.5}(H_2O)_{26}]\cdot24H_2O$ (**5**), $CsK_{2.25}[GeW_9Nb_3O_{40}Eu_{1.25}(H_2O)_{12}]\cdot8H_2O$ (**6**). In the six compounds, all the Eu[III] are selectively bonded to the surface of the closed-shell {GeW_9Nb_3O_{40}} Keggin fragments by forming Eu–O_t(Nb) bonds rather than Eu–O_t(W) bonds (O_t: terminal oxygen), which implies the high nucleophilicity of O_t(Nb). This is further explained by Density Functional Theory (DFT) calculations on $[GeW_9Nb_3O_{40}]^{7-}$ anion. The isomerization of the {GeW_9Nb_3O_{40}} fragment makes linking between {GeW_9Nb_3O_{40}} and Eu[III] more complex: the architectures of resulting products range from 0D to 1D and 2D.

Experimental section

Materials and general methods

$Cs_{6.5}K_{0.5}[GeW_9(NbO_2)_3O_{37}]\cdot6H_2O$ and $Cs_6K_{0.5}[GeW_9Nb_3O_{40}]\cdot10H_2O$ were synthesized according to the procedure described in the literature,[9a] and their powder product were used without further purifying. They were characterized by IR spectra and Elemental analysis. All other reagents were readily available from commercial sources and used as received without further purification. The IR spectra in KBr pellets were recorded in the range 400–4000 cm^{−1} with an Alpha Centaurt FT/IR spectrophotometer. Elemental analyses for Ge, Eu, W, Nb, Cs, K, and S were determined with a PLASMASPEC (I) ICP atomic emission spectrometer. Thermogravimetric analyses were carried out by using a Perkin-Elmer TGA7 instrument, with a heating rate of 10 °C min^{−1}, under a nitrogen atmosphere. Photoluminescence spectra were measured using a FLSP 920 Edinburgh instrument (Eng) with 450 W Xenon lamp monochromatized by double grating. Computational calculations were carried out using DFT methodology with the ADF 2009 program.[13] Further information about computational calculations can be found in the Supporting Information S2.†

$Cs_3K_4[(Ge_2W_{18}Nb_6O_{78})Eu(H_2O)_4]\cdot23H_2O$ (**1**).
Solid EuCl_3·6H_2O (0.051 g, 0.15 mmol) was added to a solution of $Cs_{6.5}K_{0.5}[GeW_9(NbO_2)_3O_{37}]\cdot6H_2O$ (1.0 g, 0.27 mmol) in HCl solution (0.5 M, 30 mL). The resulting clear solution was heated at reflux for 4 h and then cooled to room temperature. After a small amount of white insoluble solid had been removed by filtration, the filtrate was allowed to evaporate at room temperature. Colorless block crystals suitable for X-ray crystallography were obtained within 1 week (yield: 62%). Anal. calcd (%) for $Cs_3K_4[(Ge_2W_{18}Nb_6O_{78})Eu(H_2O)_4]\cdot23H_2O$: K, 2.42; Ge, 2.25; Nb, 8.64; Cs, 6.18; Eu, 2.35; W, 51.28; found: K, 2.39; Ge, 2.11; Nb, 8.95; Cs, 6.54; Eu, 2.68; W, 53.94. IR (KBr disks): 968 (w), 883 (vs), 810 (sh), 762 (vs), 671 (s), 528 (w), 454 (s).

$Cs_8K_9[(Ge_4W_{36}Nb_{12}O_{156})Eu(H_2O)_3]\cdot25H_2O$ (**2**).
2 was prepared following the procedure described for **1**, but by using a smaller quantity of EuCl_3·6H_2O (0.025 g, 0.07 mmol). The resulting products were colorless lamellar crystals (yield: 58%). Anal. calcd (%) for $Cs_8K_9[(Ge_4W_{36}Nb_{12}O_{156})Eu(H_2O)_3]\cdot25H_2O$: K, 2.79; Ge, 2.30; Nb, 8.85; Cs, 8.44; Eu, 1.21; W, 52.56; found: K, 2.65; Ge, 2.48; Nb, 8.55; Cs, 8.28; Eu, 1.35; W, 53.34. IR (KBr disks): 966 (w), 879 (vs), 809 (sh), 761 (vs), 671 (s), 529 (w), 456 (s).

$Cs_{12}K_2[Cs(GeW_9Nb_3O_{40})_4(SO_4)Eu_5(H_2O)_{36}]\cdot61H_2O$ (**3**).
Solid NaHSO_3 (0.1 g, 0.96 mmol) was added to a solution of $Cs_{6.5}K_{0.5}[GeW_9(NbO_2)_3O_{37}]\cdot6H_2O$ (1.0 g, 0.27 mmol) in hot water (25 mL). After the yellow solution become colorless, HCl (0.12mL, 0.5 M) was added dropwise, followed by EuCl_3 solution (0.15 g EuCl_3·6H_2O) in water (2 mL). The resulting mixture (pH 4.0) was heated to 80 °C with vigorous stirring for 2 h then cooled to room temperature. A small amount of insoluble solid was removed by filtration, and the filtrate was allowed to evaporate at room temperature. Colorless sheet crystals suitable for X-ray crystallography were obtained within 1 week (yield: 42%). Anal. calcd (%) for $Cs_{12}K_2[Cs(GeW_9Nb_3O_{40})_4(SO_4)Eu_5(H_2O)_{36}]\cdot61H_2O$: S, 0.21; K, 0.52; Ge, 1.94; Nb, 7.43; Cs, 11.52; Eu, 5.07; W, 44.14; found: S, 0.29; K, 0.64; Ge, 2.18; Nb, 7.63; Cs, 11.39; Eu, 4.88; W, 44.45. IR (KBr disks): 1109(w), 884 (s), 806 (sh), 760 (vs), 529 (vw), 458 (w).

$Cs_{12.5}K_{1.5}[Cs_2(GeW_9Nb_3O_{40})_4Eu_4(H_2O)_{22}]\cdot28H_2O$ (**4**).
A sample of $Cs_{6.5}K_{0.5}[GeW_9Nb_3O_{40}]\cdot10H_2O$ (1.0 g, 0.27 mmol) was added to a solution of EuCl_3·6H_2O (0.15 g, 0.41 mmol) in NaOAc/HOAc buffer (1.0 M, 25 mL) at pH 4.8. The resulting solution was heated at 80 °C with vigorous stirring for 2 h then cooled to room temperature. A small amount of insoluble solid was removed by filtration, and the filtrate was allowed to evaporate at room temperature. Colorless sheet crystals suitable for X-ray crystallography were obtained within 1 week (yield: 50%). Anal. calcd (%) for $Cs_{12.5}K_{1.5}[Cs_2(GeW_9Nb_3O_{40})_4Eu_4(H_2O)_{22}]\cdot28H_2O$: K, 0.42; Ge, 2.06; Nb, 7.92; Cs, 13.69; Eu, 4.32; W, 47.01; found: K, 0.31; Ge, 2.32; Nb, 7.54; Cs, 13.19; Eu, 4.03; W, 47.42. IR (KBr disks): 952 (w), 884 (s), 812 (sh), 769 (vs), 533 (vw), 458 (w).

$Cs_{11.5}[(GeW_9Nb_3O_{40})_4Eu_{5.5}(H_2O)_{26}]\cdot24H_2O$ (**5**).
HCl (0.5 M, 0.4 mL) was added to a solution of $Cs_{6.5}K_{0.5}[GeW_9(NbO_2)_3O_{37}]\cdot6H_2O$ (1.0 g, 0.27 mmol) in hot water (25 ml). EuCl_3·6H_2O (0.15 g, 0.41 mmol) in water (5 mL) was added dropwise. The final pH was adjusted to 2.2 with HCl (0.5 M). The resulting solution was heated at reflux for 5 h until the yellow solution turned to colorless, and then cooled to room temperature. After a small amount of white insoluble solid was removed by filtration, the filtrate was allowed to evaporate at room temperature. Colorless lamellar crystals suitable for X-ray crystallography were obtained within 1 week (yield: 51%). Anal. calcd (%) for

$Cs_{11.5}[(GeW_9Nb_3O_{40})_4Eu_{5.5}(H_2O)_{26}]\cdot24H_2O$: Ge, 2.10; Nb, 8.05; Cs, 11.04; Eu, 6.04; W, 47.79; found: Ge, 1.88; Nb, 7.89; Cs, 10.82; Eu, 6.31; W, 48.14. IR (KBr disks): 957 (w), 885 (s), 807 (sh), 757 (vs), 533 (vw), 453 (w).

$CsK_{2.25}[GeW_9Nb_3O_{40}Eu_{1.25}(H_2O)_{12}]\cdot8H_2O$ (6). The same procedure as that for **5** was followed, except for the final pH of 3.0. Colorless square crystals suitable for X-ray crystallography were obtained within 1 week (yield: 57%). Anal. calcd (%) for $CsK_{2.25}[GeW_9Nb_3O_{40}Eu_{1.25}(H_2O)_{12}]\cdot8H_2O$: K, 2.57; Ge, 2.13; Nb, 8.16; Cs, 3.89; Eu, 5.55; W, 48.42; found: K, 2.51; Ge, 2.34; Nb, 8.75; Cs, 3.83; Eu, 4.24; W, 50.87. IR (KBr disks): 957 (s), 885 (vs), 807 (s), 757 (vs), 531 (vw), 453 (w).

Single-crystal X-ray crystallography

Single-crystal diffractometry was conducted on a Bruker Smart Apex CCD diffractometer with Mo KR monochromated radiation ($\lambda = 0.71073$ Å) at room temperature. The linear absorption coefficients, scattering factors for the atoms, and anomalous dispersion corrections were taken from the International Tables for X-Ray Crystallography.[14] Empirical absorption corrections were applied. The structures were solved by using the direct method and refined through the fullmatrix least-squares method on F^2 using SHELXS-97.[15] Anisotropic thermal parameters were used to refine all non-hydrogen atoms, with the exception for some oxygen atoms. Those hydrogen atoms attached to lattice water molecules were not located. Crystallization water molecules were estimated by thermogravimetry and only partial oxygen atoms of water molecules were achieved with the X-ray structure analysis. The crystal data and structure refinement results of **1–6** are summarized in Table 1. Further details on the crystal structure investigations may be obtained from the Fachinformationszentrum Karlsruhe, 76344 Eggenstein-Leopoldshafen, Germany (fax: (+49) 7247-808-666; e-mail: crysdata@fiz-karlsruhe.de), on quoting the depository numbers CSD-422598 (**1**), CSD-422599 (**2**), CSD-422600 (**3**), CSD-422601 (**4**), CSD-422602 (**5**), CSD-422603 (**6**).

Results and discussion

Synthesis

As shown in Fig. 1, compounds **1** and **2** were synthesized by refluxing 0.5 M HCl solution containing different ratios of $EuCl_3$ and $Cs_{6.5}K_{0.5}[GeW_9(NbO_2)_3O_{37}]$ (the ratios are 1 : 2 for **1** and 1 : 4 for **2**). Both Nb–O–Nb and Nb–O–Eu bridges exist in the anions of **1** and **2** (**1a** and **2a**). It is known that Nb–O–Nb bridges are easily formed between two or more Nb-substituted POM molecules upon acidification.[9,11e,11f] So, there is competition between the formation of Nb–O–Nb bridges and (Nb)O–Eu bonds in acidic solution. For example, the formation of Nb–O–Nb in **1a** and **2a** consumes $O_t(Nb)$ and restricts the further combining with Eu^{III}. We performed a series of experiments under different pH conditions and the results indicate that the formation of Nb–O–Nb can be avoided only when pH>1.5 (determined by the disappearance of the Nb–O–Nb characteristic vibrations at 671 cm^{-1} in the IR spectra of the resulting production). Therefore, in the synthesis process of **3–6** the pH was increased to above 1.5. As expected, no Nb–O–Nb bridge

exists in the anions of **3–6** (**3a–6a**), and there are higher proportions of Eu^{III} in **3a–6a** than that in **1a** and **2a**.

The syntheses of **5** and **6** were performed by refluxing the solutions containing $EuCl_3$ and $Cs_{6.5}K_{0.5}[GeW_9(NbO_2)_3O_{37}]$ at pH 3.0 for **5** and 2.2 for **6** (Fig. 1). Farther increasing the pH of the solution containing $EuCl_3$ and $Cs_{6.5}K_{0.5}[GeW_9(NbO_2)_3O_{37}]$ resulted in fierce deposition. Thus, we attempted to use the peroxo-free $[GeW_9Nb_3O_{40}]^{7-}$ (reduced by $NaHSO_3$) as starting material in the syntheses of **3** and **4** (Fig. 1). **3** was synthesized at pH 4.0 from the reaction $[GeW_9Nb_3O_{40}]^{7-}$ and $EuCl_3$. **4** was synthesized by utilizing $Cs_{6.5}K_{0.5}[GeW_9Nb_3O_{40}]$ and Eu^{3+} in NaOAc/AcOH buffer (1.0 M, pH 4.8).

The facile formation of Nb–O–Eu bridges in compounds **1–6** indicates the high reaction activity of $[GeW_9Nb_3O_{40}]^{7-}$ towards oxophilic lanthanide. It is known that Lacunary POT precursors are usually sensitive to pH value and sometimes undergo the courses of disassembly and reassembly in the reaction process.[16] However, the $\{GeW_9Nb_3O_{40}\}$ precursor has been retained in all six compounds. Therefore, the closed-shell mixed-addendum POMs are not only active but also more stable in retaining the structure type (Keggin type herein) under a broad pH range.

Owing to the large ionic radius, lanthanide ions usually connect with POMs though weak Ln–O(POM) linkages, and the resulting structures are sometimes opened and fragile.[1d,17] As shown in Figure S1.1†, Cs^+ cations fill in the gaps of the polyanions **1–5** and coordinate to their surface oxygen, which make these polyanions much firmer. The flexible Cs^+ coordination and the alterable Cs–O distance may render Cs^+ play an important templating role in the formation and stability of polyanions **1a–5a**. This is also evidenced by the experimental results that no identifiable products could be obtained in the absence of Cs^+ ions.

Structure description

The anion of **1** (**1a**) with C_{2v} symmetry is composed of two $\{GeW_9Nb_3O_{40}\}$ fragments which are linked together *via* two Nb–O–Nb bridges and one $(Nb)O_t$–Eu–$O_t(Nb)$ bridge (Fig. 2a). The Eu^{III} coordination character of **1a** affords capacious space for further derivatization. The anion of **2** (**2a**) is a tetramer composed of four $\{GeW_9Nb_3O_{40}\}$ and a central Eu^{III} (Fig. 2b). Alternatively, **2a** can be regarded as a derivative of **1a** whose two aqua ligands on Eu^{III} are substituted by two $O_t(Nb)$ from another $\{Ge_2W_{18}Nb_6O_{78}\}$ fragment.

Interestingly, the anions of **3–5** (**3a–5a**) are all made up of telephone receiver-like building units "$(GeW_9Nb_3O_{40})_2Eu_2$" (abbreviated "Telephone units"). As shown in Fig. S1.2.1† the C_{2v} symmetric Telephone unit contains two $\{GeW_9Nb_3O_{40}\}$ segments in which adjacent four $O_t(Nb)$ atoms from two Nb_3O_{13} clusters are connected by two Eu^{III}. As a result of the different coordinate of the other two $O_t(Nb)$, the Telephone units are linked to different architectures in **3a–5a** (Fig. S1.2.2 and S1.2.3†).

As shown in Fig. 3a, in polyanion **3a** two Telephone units are linked by two Eu^{III} *via* $O_t(Nb)$–Eu–$O_t(Nb)$ bridges, forming a quadrangular molecule. In a Telephone unit of **3a**, one of the Eu^{III} is replaced by an eleven-coordinate Cs^+, so the symmetry of the quadrangle reduces from D_{2h} to C_s. A sulfate ion (rooting in the oxidation of $NaHSO_3$ by the peroxo groups of the precursor)

Table 1 Crystal data and structural refinement for compounds **1–6**

Compound	1	2	3	4	5	6
Formula	$Cs_3EuGe_2H_{54}$-$K_4Nb_6O_{105}W_{18}$	$Cs_8EuGe_4H_{56}$-$K_9Nb_{12}O_{184}W_{36}$	$Cs_{13}Eu_5Ge_4H_{194}$-$K_2Nb_{12}O_{261}SW_{36}$	$Cs_{14.5}Eu_4Ge_4H_{100}$-$K_{1.5}Nb_{12}O_{210}W_{36}$	$H_{100}Cs_{11.5}Ge_4$-$Nb_{12}Eu_{5.5}W_{36}O_{210}$	$H_{40}K_{2.25}CsGe$-$Nb_3Eu_{1.25}W_9O_{60}$
Formula weight (g mol^{-1})	6453.28	12591.10	14992.91	14077.98	13848.56	3417.03
T (K)	296 (2)	296 (2)	296 (2)	296 (2)	296 (2)	296 (2)
Wavelength (Å)	0.71073	0.71073	0.71073	0.71073	0.71073	0.71073
Crystal system	Monoclinic	Triclinic	Triclinic	Triclinic	Triclinic	Orthorhombic
Space group	$C2/m$	$P\bar{1}$	$P\bar{1}$	$P\bar{1}$	$P\bar{1}$	Pnma
a (Å)	34.287(5)	12.886(5)	12.767(5)	12.792(5)	13.408(5)	28.9984(17)
b (Å)	16.423(5)	19.278(5)	22.821(5)	22.171(5)	21.274(5)	17.0329(8)
c (Å)	21.686(5)	21.083(5)	43.145(5)	23.875(5)	22.017(5)	12.5949(5)
α (°)	90	77.176	80.860(5)	64.318(5)	96.138(5)	90.00
β (°)	114.365	76.762(5)	84.128(5)	75.091(5)	105.057(5)	90.00
γ (°)	90	82.918(5)	85.375(5)	81.977(5)	90.214(5)	90.00
V (Å^3)	11124(5)	4957(3)	12319(6)	5894(3)	6027(3)	6221.0(5)
Z	4	1	2	1	1	4
D_{calc} (mg m^{-3})	3.853	4.225	4.042	3.928	3.779	3.648
μ (mm^{-1})	21.415	24.101	21.046	21.921	21.347	19.681
$F(000)$	10808.0	5468.4	12704.0	6031.6	5927.0	5562.9
Crystal size (mm)	$0.20 \times 0.18 \times 0.18$	$0.22 \times 0.22 \times 0.10$	$0.24 \times 0.20 \times 0.08$	$0.25 \times 0.18 \times 0.07$	$0.22 \times 0.22 \times 0.18$	$0.24 \times 0.24 \times 0.04$
Goodness–of–fit on F^2	1.035	1.002	1.011	1.020	1.090	1.035
Final R indices $[I > 2\sigma(I)]^a$	$R_1 = 0.0521$ wR$_2 = 0.1381$	$R_1 = 0.0628$ wR$_2 = 0.1564$	$R_1 = 0.0535$ wR$_2 = 0.1344$	$R_1 = 0.1045$ wR$_2 = 0.2698$	$R_1 = 0.0826$ wR$_2 = 0.2511$	$R_1 = 0.0586$ wR$_2 = 0.1361$
R indices^a (all data)	$R_1 = 0.0895$ wR$_2 = 0.1540$	$R_1 = 0.1127$ wR$_2 = 0.1760$	$R_1 = 0.0682$ wR$_2 = 0.1412$	$R_1 = 0.1349$ wR$_2 = 0.2890$	$R_1 = 0.1238$ wR$_2 = 0.2784$	$R_1 = 0.1146$ wR$_2 = 0.1419$

^{a} $R_1 = \sum ||F_o| - |F_c||\sum|F_o|$; wR$_2 = \{\sum[w(F_o^2 - F_c^2)^2]/\sum[w(F_o^2)^2]\}^{1/2}$.

bridges the Cs$^+$ and an adjacent Eu^{III} with average S–O distance of 1.49 Å. Polyanion **4a** is also a tetramer with idealized C_i symmetry (Fig. 3b). It is constructed by two equal Telephone units, which are further connected together by two O$_t$(Nb)–Eu–O$_t$(Nb) bridges and two O(Nb)–Cs–O(W) bridges, forming a parallelogram.
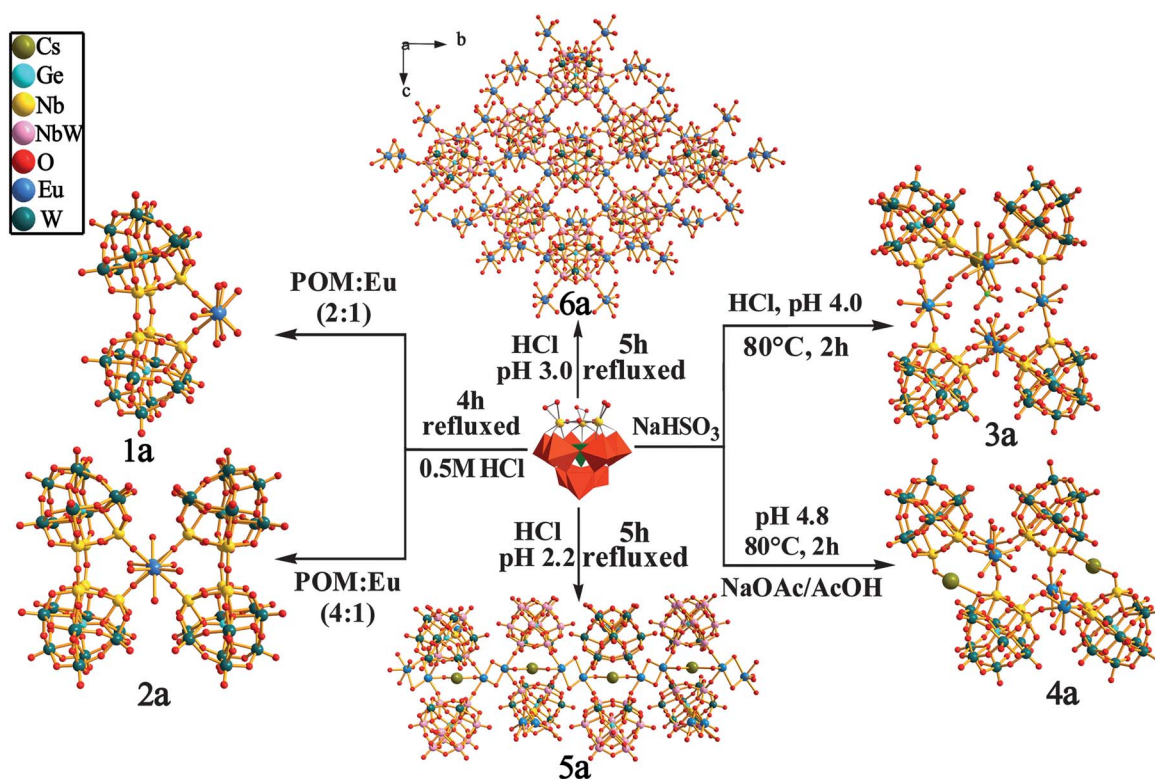
Fig. 1 Synthesis routes for compounds **1–6** (they are represented by their anions **1a–6a** respectively).

This journal is © The Royal Society of Chemistry 2012
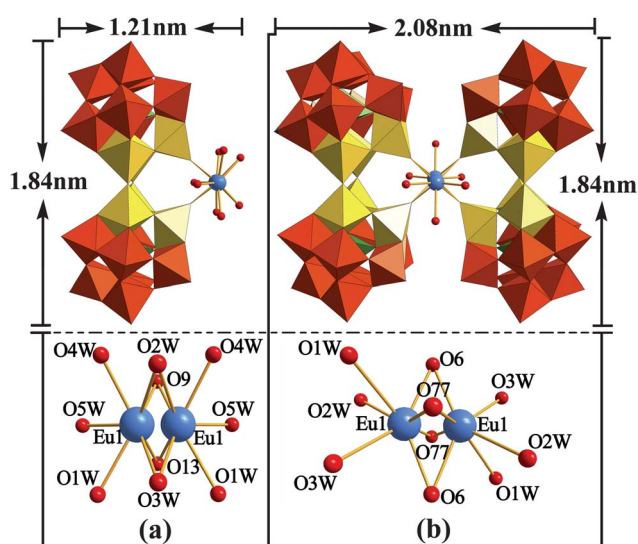
Fig. 2 Combined polyhedral/ball-and-stick representation of **1a** (a top), and **2a** (b top), and the coordination environments for Eu^{3+} in **1a** (a bottom) and **2a** (b bottom). WO$_6$ octahedra (red), NbO$_6$ octahedra (golden), GeO$_4$ tetrahedrons (green). The balls represent: europium (blue), oxygen (red), cesium (dark yellow).

Fig. 3 Combined polyhedral/ball-and-stick representation of **3a** (a), and **4a** (b). The bright green ball represents sulfur.

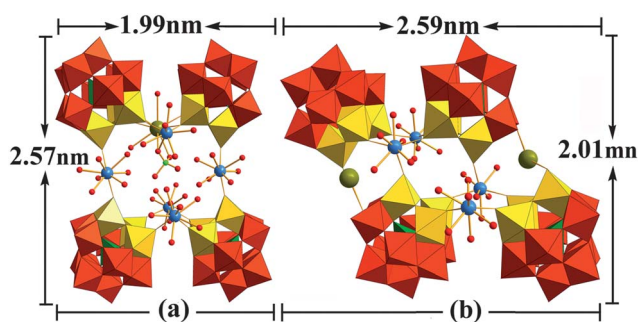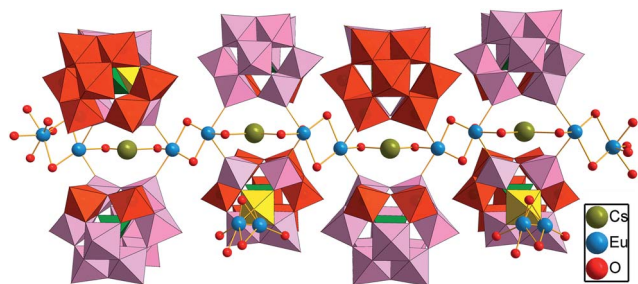In polyanion **5a**, the Telephone units are linked to a 1D chain by sharing aqua ligands of adjacent Eu^{III} (Fig. 4 and Fig. S1.3.2†). It is noteworthy that there are serious crystallographic disorders in the two {GeW$_9$Nb$_3$O$_{40}$} fragments of the Telephone unit of **5a** (Fig. S1.3.1†). In polyanion **6a**, three Nb

Fig. 4 Representation of the 1D chain for **5a**. Partial aqua ligands on Eu^{III} are omitted for clarity. The color code is the same as in Fig. 2, and the rose octahedra represent W/NbO$_6$ (in which W and Nb are disordered).

atoms are disordered over nine positions of the {GeW$_9$Nb$_3$O$_{40}$} Keggin fragment, with an occupancy factor of 1 : 2 for Nb : W. Interestingly, all nine O$_t$(Nb/W) are linked to Eu^{III} resulting in a 2D layer structure (Fig. 5a and Fig. S1.3.3†). There are two kinds of crystallographically independent Eu^{III} atoms in **6a** labeled as Eu1 and Eu2 in Fig. 5b and 4c. Every Eu1 atom is seven-coordinate and links to three {GeW$_9$Nb$_3$O$_{40}$} fragments with average Eu–O$_t$(Nb/W) bond length of 2.39 Å. Every nine-coordinated Eu2 is disordered in two positions and links to three {GeW$_9$Nb$_3$O$_{40}$} with average Eu–O$_t$(Nb/W) distance of 2.55 Å.

Similar to other substituted-type POMs, in the [GeW$_9$Nb$_3$O$_{40}$]$^{7-}$ anion three Nb atoms are disordered upon twelve metal positions.[9,18] The grafting of Eu^{III} to {GeW$_9$Nb$_3$O$_{40}$} restricts the random orientational disorder: other four isomers of {GeW$_9$Nb$_3$O$_{40}$} are found in the six
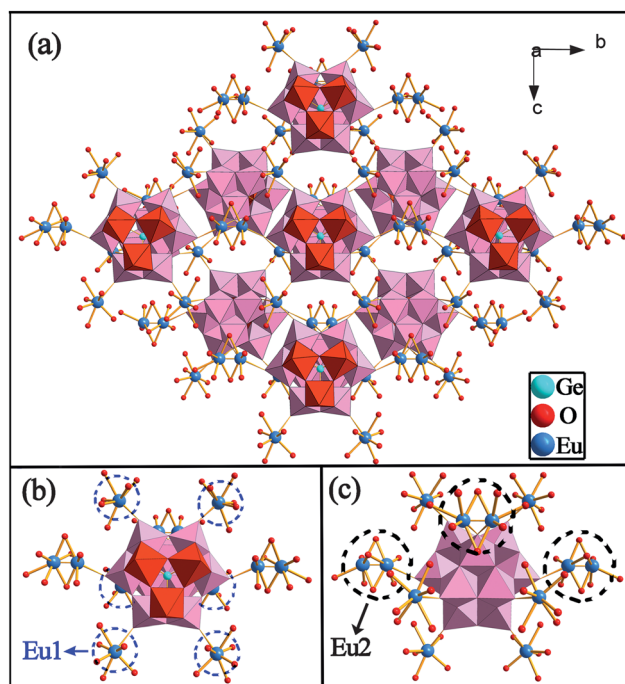
Fig. 5 Representation of 2D layer for **6a** (a); and the linking between one {GeW$_9$Nb$_3$O$_{40}$} and nine Eu atoms, viewing from the top (b) and bottom (c). The color code is the same as in Fig. 2 and Fig. 4.

compounds (Fig. S1.3.4†). The selective connection of Eu^{III} with O$_t$(Nb) or O$_t$(Nb/W) from these isomers results in various architectures of the products.

Density functional theory (DFT) calculations

DFT calculations provide intelligible reasons why the Eu^{III} are selectively connected to O$_t$(Nb). The Molecular Electrostatic Potentials (MEPs) distribution for [GeW$_9$Nb$_3$O$_{40}$]$^{7-}$ (Fig. 6) illustrates that the Nb$_3$O$_{13}$ cluster is indeed the potential nucleophilic center of the Keggin anion. Furthermore, the Mulliken charge analysis of the surface O atoms of [GeW$_9$Nb$_3$O$_{40}$]$^{7-}$ (Table S1†) suggests the following oxygen basicity scale: O$_b$(Nb$_2$) > O$_b$(NbW) > O$_b$(W$_2$) > O$_t$(Nb) > O$_t$(W), and the basicity of O$_t$(Nb) is obviously stronger than that of O$_t$(W). Though

bridging oxygen (O_b) possess higher nucleophilicity, no Eu–O_b(Nb_2) or Eu–O_b(NbW) bond is observed in the experimental results. That perhaps due to the steric hindrance of {$GeW_9Nb_3O_{40}$} and coordination character of Eu^{III}.

Photoluminescence properties

The solid photoluminescence behaviors of **1–6** have been investigated at room temperature. They all exhibit the characteristic transition of Eu^{III} under the excitation wavelength (394 nm). The solid emission spectra of **1** and **2** (as shown in Fig. 7 and Fig. S3.2†) both exhibit the characteristic transition of the Eu^{III} at 579, 592, 614, 651 and 699 nm corresponding to the $^5D_0 \rightarrow {}^7F_J$ (J = 0–4) transitions, respectively. The $^5D_0 \rightarrow {}^7F_0$ transition corresponds to the symmetry-forbidden emission, which is strictly forbidden in a field of symmetry. The presence of $^5D_0 \rightarrow {}^7F_0$ transition in **1** reveals that site symmetry of the Eu^{III} is low without an inversion center in **1**. However the $^5D_0 \rightarrow {}^7F_0$ transition of **2** can hardly be observed, indicating the comparatively higher symmetry. The $^5D_0 \rightarrow {}^7F_1$ and $^5D_0 \rightarrow {}^7F_2$ transitions are ascribed to the magnetic and electric dipole transitions, respectively. The former mainly depends on the ligand field strength acting on Eu^{III} and is fairly insensitive to the coordination environment of the Eu^{III}. While the latter that corresponds to the strongest emission at 614 nm, is greatly sensitive to chemical bonds in the vicinity of the Eu^{III}; it increases as the site symmetry of Eu^{III} center decreases. Consequently, the I($^5D_0 \rightarrow {}^7F_2$)/I($^5D_0 \rightarrow {}^7F_1$) ratio is widely used as a measurement of the coordination state and site symmetry of lanthanide.[1b,19] This ratios of compound **1** and **2** are 7.25 and 6.22, respectively, which indicates the lower site symmetry of Eu^{III} in **1** than **2**. This is also in agreement with the results of the single-crystal X-ray analysis for **1** and **2**. The solid emission spectra of **3–6** show similar character with that of **1**.

The solution photoluminescence spectra of **1** and **2** exhibit uniform manner with that in the solid state, indicating uniform coordination environment in solid and solution states. The emission spectra of **1** and **2** have been monitored in the presence
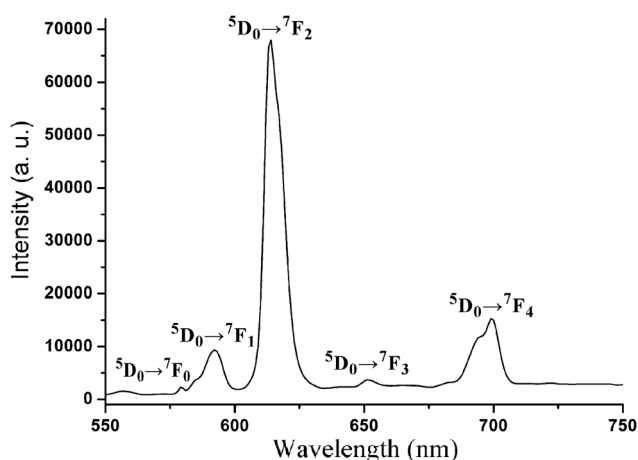
Fig. 7 Emission spectrum (λ_{ex} = 394 nm) of solid sample **1**.

of various carboxylic acids including acetate, oxalic, malonic and succinic acids. No obvious changes take place in the emission spectra of **2** for the presence of all four carboxylic acids. However, the emission intensity of **1** increases remarkably with the addition of malonic acid. The introduction of the other three carboxylic acids to **1** does not bring obvious changes to the emission spectra (Fig. 8). It has been reported that the coordinated water on Ln^{III} is facilely substituted by organic ligands in aqueous solution and this can enhance the luminescence intensity and prolong lifetime of Eu^{III} species.[20] As shown in Fig. S3.4 and S3.5, the emission lifetime of **1** reaches to 0.21 ms after adding 1.2 equiv. of malonic acid, which is substantially longer than that without malonic acid (0.13 ms). The luminescent response herein may be rationalized by considering the substitution of coordinated water by the polarizable C–O donors of malonic acid in solution state. But why the substitution exclusively occurs between **1** and malonic acid? This is perhaps owing to the suited architectural feature (as shown in Fig. S3.6†), which is conducive to the simultaneous substitution of the two terminal aqua ligands of **1a** by the two carboxyl groups of one malonic acid molecule resulting in a six-membered chelate ring. Unfortunately, the crystal data of malonic acid-coordinated **1a** was not obtained by far. And attempts to detect the production by ESI-MS experiments did not give any meaningful results. Further research on luminescent mechanism and the derivatization of **1a** can be expected in future work.

Conclusions

It has been demonstrated by experimental and computational methods that W/Nb mixed-addendum POMs are active towards lanthanide. It is the first time for the combination of lanthanide and niobate under conventional acidic conditions. Six (Nb)O–Eu bond-based POMs (including 0D, 1D, and 2D structures) have been isolated. Compared with the (Nb)O–Eu bonds, the formation of Nb–O–Nb bridges needs stronger acidity. Thus, weaker acidity (pH > 1.5) is favorable to the former. The closed-shell mixed-addendum POMs are not only comparable to lacunary POTs in activity, but also more stable in retaining the structure type under a broad pH range. Hence, the reactions that took place in the Lacunary POTs are expected to be carried out in the Mixed-addendum POMs.
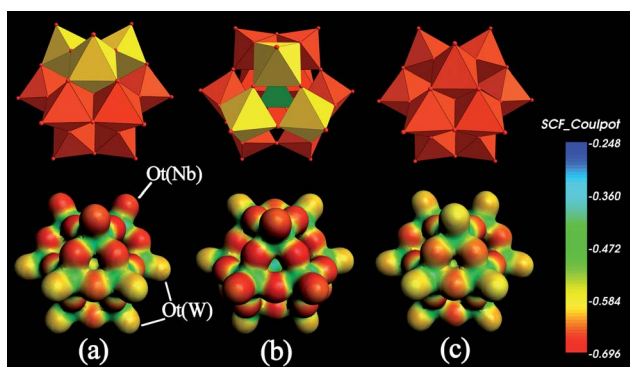
Fig. 6 Molecular Electrostatic Potentials (MEPs) from three different viewpoints of the 3D surface (bottom) and corresponding polyhedral representations (top) for [$GeW_9Nb_3O_{40}$]$^{7-}$ anion. The color of the electronic density isosurface (ρ = 0.022 e/ua) is a function of the MEP value. In the figures, red regions represent nucleophilic areas where the electrostatic potential is negative and green regions represent electrophilic areas which possess positive or less negative electrostatic potential. The color code in the polyhedral representations is the same as in Fig. 2.
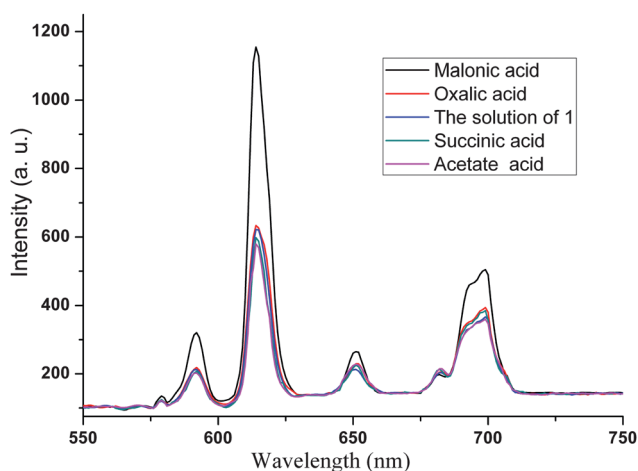
Fig. 8 The luminescence spectra of **1** (1.0×10^{-3} M, in 0.5M HCl solution) upon addition of acetate acid, oxalic acid, malonic acid and succinic acids (1.0 equal, excited at 394 nm).

A series of niobium-substituted POMs with different frames and Nb/W rates may be prepared and utilized to connect lanthanides by the formation of (Nb)O–Ln bonds, so a new enormous (Nb)O–Ln bond-based POMs family can be constructed. Derivatization on the labile terminal aqua ligands of lanthanides will make this family more flourishing. The combination of Nb/W mixed-addendum POMs with other electrophilic species including transition metals and water-soluble metal-lorganic complexes may be achieved. Not only POMs of Nb/W system, other Early Transition Metal Mixed-addendum POMs (ETMMPs, for example Ta/W and Ti/W systems) may also be available for the above-mentioned likelihood.

Acknowledgements

Notes and references

1 (a) A. Müller, F. Peters, M. T. Pope and D. Gatteschi, *Chem. Rev.*, 1998, **98**, 239; (b) T. Yamase, *Chem. Rev.*, 1998, **98**, 307; (c) D. L. Long, E. Burkholder and L. Cronin, *Chem. Soc. Rev.*, 2007, **36**, 105; (d) B. S. Bassil and U. Z. Kortz, *Z. Anorg. Allg. Chem.*, 2010, **636**, 2222.
2 (a) C. Ritchie, E. G. Moore, M. Speldrich, P. Kögerler and C. Boskovic, *Angew. Chem., Int. Ed.*, 2010, **49**, 7702; (b) M. A. AlDamen, J. M. Clemente-Juan, E. Coronado, C. Martí-Gastaldo and A. Gaita-Ariño, *J. Am. Chem. Soc.*, 2008, **130**, 8874; (c) C. Boglio, G. Lemière, B. Hasenknopf, S. Thorimbert, E. Lacôte and M. Malacria, *Angew. Chem., Int. Ed.*, 2006, **45**, 3324; (d) C.-D. Wu, C.-Z. Lu, H.-H. Zhuang and J.-S. Huang, *J. Am. Chem. Soc.*, 2002, **124**, 3836; (e) S. X. Liu, D. H. Li, L. H. Xie, H. Y. Cheng, X. Y. Zhao and Z. M. Su, *Inorg. Chem.*, 2006, **45**, 8036.
3 R. D. Peacock and T. J. R. Weakley, *J. Chem. Soc. A*, 1971, 1836.
4 (a) B. S. Bassil, M. H. Dickman, I. Römer, B. Kammer and U. Kortz, *Angew. Chem., Int. Ed.*, 2007, **46**, 6192; (b) F. Hussain, F. Conrad and G. R. Patzke, *Angew. Chem., Int. Ed.*, 2009, **48**, 9088; (c) F. Hussain, R. W. Gable, M. Speldrich, P. Kögerlerb and C. Boskovic, *Chem. Commun.*, 2009, 328; (d) K. Wassermann, M. H. Dickman and M. T. Pope, *Angew. Chem., Int. Ed.*, 1997, **36**, 1445; (e)

M. Zimmermann, N. Belai, R. J. Butcher, M. T. Pope, E. V. Chubarova, M. H. Dickman and U. Kortz, *Inorg. Chem.*, 2007, **46**, 1737; (f) F. Hussain and G. R. Patzke, *CrystEngComm*, 2011, **13**, 530; (g) K. Fukaya and T. Yamase, *Angew. Chem., Int. Ed*, 2003, **42**, 654; (h) T. Yamase, H. Naruke and Y. Sasaki, *J. Chem. Soc., Dalton Trans.*, 1990, 1687.
5 (a) B. S. Bassil, M. H. Dickman, B. Kammer and U. Kortz, *Inorg. Chem.*, 2007, **46**, 2452; (b) C. Zhang, R. C. Howell, K. B. Scotland, F. G. Perez, L. Todaro and L. C. Francesconi, *Inorg. Chem.*, 2004, **43**, 7691; (c) M. N. Sokolova, A. M. Fedosseev, G. B. Andreev, N. A. Budantseva, A. B. Yusov and P. Moisy, *Inorg. Chem.*, 2009, **48**, 9185; (d) W. L. Chen, Y. G. Li, Y. H. Wang, E. B. Wang and Z. M. Su, *Dalton Trans.*, 2007, 4293; (e) J. Y. Niu, K. H. Wang, H. N. Chen, J. W. Zhao, P. T. Ma, J. P. Wang, M. L. Li, Y. Bai and D. B. Dang, *Cryst. Growth Des.*, 2009, **9**, 4362.
6 (a) M. R. Antonio, M. Nyman and T. M. Anderson, *Angew. Chem., Int. Ed.*, 2009, **48**, 6136; (b) T. M. Anderson, S. G. Thoma, F. Bonhomme, M. A. Rodriguez, H. Park, J. B. Parise, T. M. Alam, J. P. Larentzos and M. Nyman, *Cryst. Growth Des.*, 2007, **7**, 719; (c) R. P. Bontchev, E. L. Venturini and M. Nyman, *Inorg. Chem.*, 2007, **46**, 4483; (d) J. Y. Niu, P. T. Ma, H. Y. Niu, J. Li, J. W. Zhao, Y. Song and J. P. Wang, *Chem.–Eur. J.*, 2007, **13**, 8739; (e) J. Y. Niu, G. Chen, J. W. Zhao, P. T. Ma, S. Z. Li, J. P. Wang, M. X. Li, Y. Bai and B. S. Ji, *Chem.–Eur. J.*, 2010, **16**, 7082.
7 (a) M. Nyman, F. Bonhomme, T. M. Alam, J. B. Parise and G. M. B. Vaughan, *Angew. Chem., Int. Ed.*, 2004, **43**, 2787; (b) M. Nyman, F. Bonhomme, T. M. Alam, M. A. Rodriguez, B. R. Cherry, J. L. Krumhansl, T. M. Nenoff and A. M. Sattler, *Science*, 2002, **297**, 996.
8 T. Ozeki, T. Yamase, H. Naruke and Y. Sasaki, *Inorg. Chem.*, 1994, **33**, 409.
9 (a) S. J. Li, S. X. Liu, C. C. Li, F. J. Ma, D. D. Liang, W. Zhang, R. K. Tan, Y. Y. Zhang and L. Xu, *Chem.–Eur. J.*, 2010, **16**, 13435; (b) G. S. Kim, H. Zeng, W. A. Neiwert, J. J. Cowan, D. VanDerveer, C. L. Hill and I. A. Weinstock, *Inorg. Chem.*, 2003, **42**, 5537; (c) S. J. Li, S. X. Liu, C. C. Li, F. J. Ma, W. Zhang, D. D. Liang, R. K. Tan, Y. Y. Zhang and Q. Tang, *Inorg. Chim. Acta*, 2011, **376**, 296.
10 (a) C. J. Besecker, V. W. Day, W. G. Klemperer and M. R. Thompson, *Inorg. Chem.*, 1985, **24**, 44; (b) F. Bannani, R. Thouvenot and M. Debbabi, *Eur. J. Inorg. Chem.*, 2007, 4357; (c) H. Driss, K. Boubekeur, M. Debbabi and R. Thouvenot, *Eur. J. Inorg. Chem.*, 2008, 3678.
11 (a) M. Dabbabi and M. Boyer, *J. Inorg. Nucl. Chem.*, 1976, **38**, 1011; (b) R. G. Finke and M. W. Droege, *J. Am. Chem. Soc.*, 1984, **106**, 7274; (c) E. V. Radkov, V. G. Young Jr and R. H. Beer, *J. Am. Chem. Soc.*, 1999, **121**, 8953; (d) D. A. Judd, Q. Chen, C. F. Campana and C. L. Hill, *J. Am. Chem. Soc.*, 1997, **119**, 5461; (e) M. K. Harrup, G.-S. Kim, H. Zeng, R. P. Johnson, D. VanDerveer and C. L. Hill, *Inorg. Chem.*, 1998, **37**, 5550; (f) G. S. Kim, H. Zeng, D. VanDerveer and C. L. Hill, *Angew. Chem., Int. Ed.*, 1999, **38**, 3205.
12 (a) V. W. Day and W. G. Klemperer, *Science*, 1985, **228**, 533; (b) C. J. Besecker, V. W. Day, W. G. Klemperer and M. R. Thompsod, *J. Am. Chem. Soc.*, 1984, **106**, 4125; (c) V. W. Day, W. G. Kiemperer and D. J. Maltbie, *Organometallics*, 1985, **4**, 104; (d) D. J. Edlund, R. J. Saxton, D. K. Lyon and R. G. Finke, *Organometallics*, 1988, **7**, 1692; (e) J. D. Aiken, Y. Lin and R. G. Finke, *J. Mol. Catal. A: Chem.*, 1996, **114**, 29.
13 Amsterdam Density Functional (ADF) Code 2009.01, Release (Vrije Universiteit, Amsterdam, The Netherlands 2009).
14 *International Tables for X-ray Crystallography*, Ed. N. F. M. Henry, K. Lonsdale, Kynoch Press, Birmingham, 1952.
15 G. M. Sheldrick, *SHELXS-97: Programs for Crystal Structure Solution*, University of Göttingen, Göttingen (Germany), 1997.
16 (a) C. Ritchie and C. Boskovic, *Cryst. Growth Des.*, 2010, **10**, 488; (b) S. T. Zheng, J. Zhang, J. M. Clemente-Juan, D. Q. Yuan and G. Y. Yang, *Angew. Chem., Int. Ed.*, 2009, **48**, 7176; (c) J. W. Zhao, C. M. Wang, J. Zhang, S. T. Zheng and G. Y. Yang, *Chem.–Eur. J.*, 2008, **14**, 9223; (d) L. H. Bi, U. Kortz, B. Keita, L. Nadjo and H. Borrmann, *Inorg. Chem.*, 2004, **43**, 8367.
17 (a) S. Reinoso, M. Giménez-Marqués, J. R. Galán-Mascarós, P. Vitoria and J. M. Gutiérrez-Zorrilla, *Angew. Chem., Int. Ed.*, 2010, **49**, 8384; (b) F. Hussain, B. Spingler, F. Conrad, M. Speldrich, P. Kögerler, C. Boskovic and G. R. Patzke, *Dalton Trans.*, 2009, 4423.

18 (*a*) G. S. Kim, H. Zeng, J. T. Rhule, I. A. Weinstock and C. L. Hill, *Chem. Commun.*, 1999, 1651; (*b*) F. Bannani, H. Driss, R. Thouvenot and M. Debbabi, *J. Chem. Crystallogr.*, 2007, **37**, 37.

19 (*a*) Q. H. Xu, L. S. Li, X. S. Liu and R. R. Xu, *Chem. Mater.*, 2002, **14**, 549; (*b*) H. He, G. J. Cao, S. T. Zheng and G. Y. Yang, *J. Am. Chem. Soc.*, 2009, **131**, 15588; (*c*) X. L. Wang, Y. Q. Guo, Y. G. Li, E. B. Wang, C. W. Hu and N. H. Hu, *Inorg. Chem.*, 2003, **42**, 4135; (*d*) T. Yamase, T. Kobayashi, M. Sugeta, H. and Naruke, *J. Phys. Chem. A*, 1997, **101**, 5046; (*e*) X. F. Li, T. F. Liu, Q. P. Lin and R. Cao, *Cryst. Growth Des.*, 2010, **10**, 608.

20 (*a*) D. Parker, R. S. Dickins, H. Puschmann, C. Crossland and J. A. K. Howard, *Chem. Rev.*, 2002, **102**, 1977; (*b*) B. L. Chen, S. C. Xiang and G. D. Qian, *Acc. Chem. Res.*, 2010, **43**, 1115; (*c*) T. Gunnlaugsson, J. P. Leonard, K. Sénéchal and A. J. Harte, *J. Am. Chem. Soc.*, 2003, **125**, 12062; (*d*) Z. Pálinkás, A. Roca-Sabio, M. Mato-Iglesias, D. Esteban-Gómez, C. Platas-Iglesias, A. de Blas, T. Rodríguez-Blas and É Tóth, *Inorg. Chem.*, 2009, **48**, 8878; (*e*) J. I. Bruce, R. S. Dickins, L. J. Govenlock, T. Gunnlaugsson, S. Lopinski, M. P. Lowe, D. Parker, R. D. Peacock, J. J. B. Perry, S. Aime and M. Botta, *J. Am. Chem. Soc.*, 2000, **122**, 9674.